MONITORING AND CONTROLLING OF STRAIN DURING MOCVD OF AlGaN FOR UV OPTOELECTRONICS

Jung Han*, M. H. Crawford, R. J. Shul, S. J. Hearne, E. Chason
J. J. Figiel, and M. Banas

Sandia National Laboratories, Albuquerque, NM 87185

Cite this article as: MRS Internet J. Nitride Semicond. Res. 4S1, G7.7 (1999)

ABSTRACT

The grown-in tensile strain, due to a lattice mismatch between AlGaN and GaN, is responsible for the observed cracking that seriously limits the feasibility of nitride-based ultraviolet (UV) emitters. We report *in-situ* monitoring of strain/stress during MOCVD of AlGaN based on a wafer-curvature measurement technique. The strain/stress measurement confirms the presence of tensile strain during growth of AlGaN pseudomorphically on a thick GaN layer. Further growth leads to the onset of stress relief through crack generation. We find that the growth of AlGaN directly on low-temperature (LT) GaN or AlN buffer layers results in a reduced and possibly controllable strain.

INTRODUCTION

Thus far the optoelectronic effort of the III-nitride community has focused primarily on InGaN-based visible light emitting devices for display and data storage applications [1]. Most of these devices were grown on sapphire substrates with thick GaN layers of 2 to 4 μms inserted for improved structural and morphological quality. (Thick n-GaN layers are also required for low-resistive electrical injection.) The active region typically consists of (higher fraction) InGaN-based quantum wells (QWs) and (lower fraction) InGaN barriers for electrical confinement. Further electrical and optical confinement is attained through the use of wide bandgap AlGaN layers (Figure 1a). Substantial lattice mismatches, however, exist among the III-nitrides; the mismatches (in the in-plane lattice constant) of InN (a ~ 0.354 nm) and AlN (a = 0.3112 nm) to the thick and presumably relaxed GaN (a = 0.3188 nm) layers are 11% compression and 2.4% tension, respectively [2]. So far most of the strain-related studies have focused on the optical [3] and structural [4] properties of thick GaN epilayers on sapphire or SiC substrates.

A simple analysis of the state of strain energy, denoted here as strain-thickness product in Figure 1c, reveals the benefit of the alternating AlGaN/InGaN heterolayers (Figure 1a) in balancing the tensile and compressive components to avoid excessive strains and to maintain a pseudomorphic growth (dashed line in Figure 1c). Recently we have reported the growth and device operation of an AlGaN/GaN QW-based UV LED on a thick GaN layer [5]. The use of various AlGaN confinement layers, in the absence of any InGaN layers (Figure 1b), results in a steep accumulation of grown-in tensile strain (solid line in Figure 1c). Indeed cracking was

* Corresponding author. Present address: Sandia National Laboratories, MS-0601, P.O. Box 5800, Albuquerque, New Mexico 87185-0601, Fax: 505-844-3211, email: jhan@sandia.gov

observed during fabrication of AlGaN/GaN UV LEDs with thick AlGaN barriers (Figure 2a). The presence of cracking causes a significant variation of current-voltage characteristics among the tested devices and contributes to a large leakage current under reverse-bias conditions (Figure 2b). It is worth noting that cracking of AlGaN layers on thick GaN has been reported previously [6, 7].

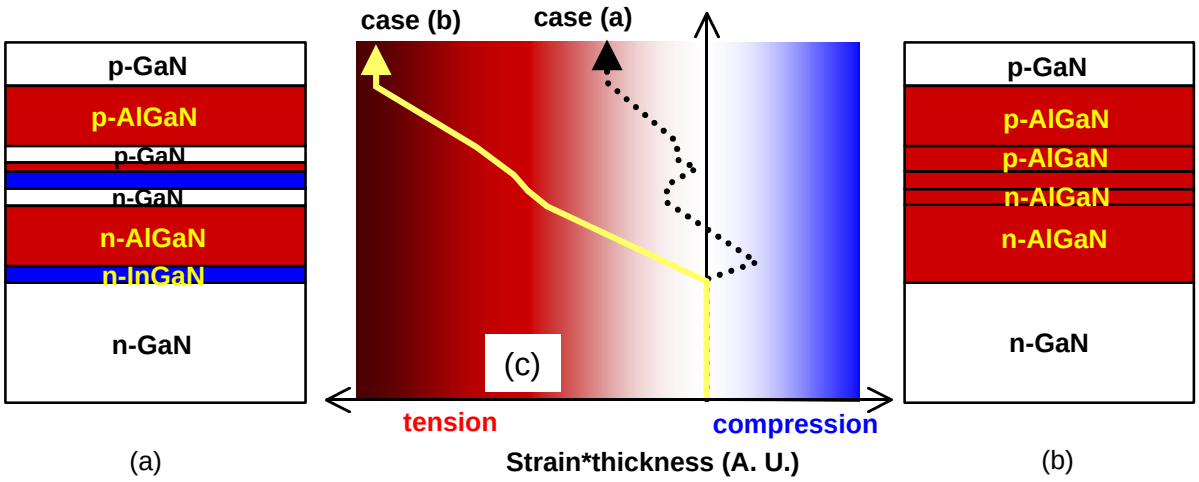

Figure 1. Schematic diagrams of a blue laser diode (a) and a UV LED (b). The indium-containing layers are labeled in blue and the AlGaN layers are colored in red. (c) Strain-thickness product along the growth direction for the structures of (a) (dashed line) and (b) (solid yellow line). InGaN layers tend to move the curve toward blue (compression) and AlGaN layers to red (tension).

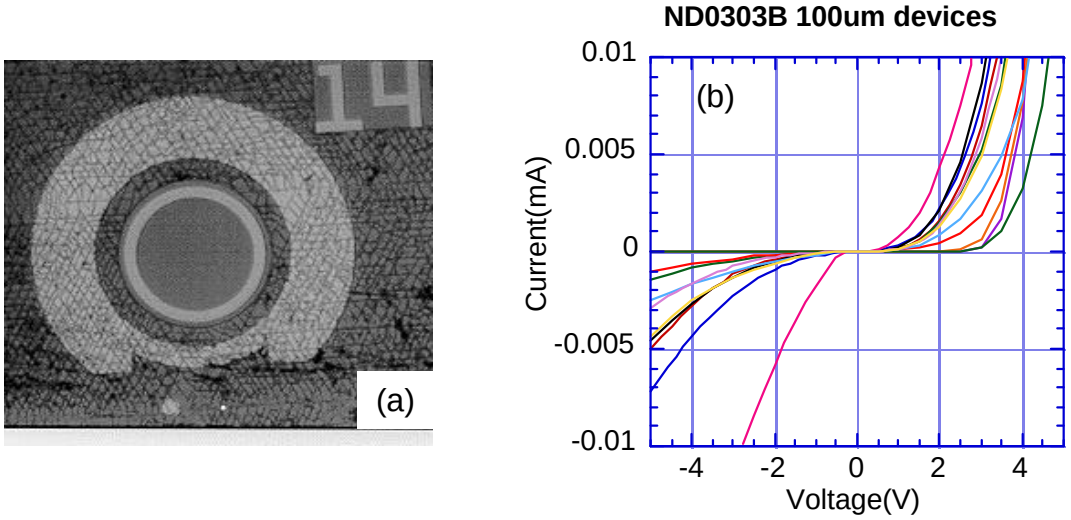

Figure 2. (a) Top view of an etched circular mesa (100 μm diameter) showing the presence of a high density of cracks. (b) Diode I-V curves taken from various devices across the same cracked sample.

An additional complication arises for AlGaN grown on sapphire, the most common substrate of choice, as the sapphire (linear thermal expansion coefficient $\alpha \sim 7.6 \times 10^{-6}\ k^{-1}$) exerts a compressive strain to the AlGaN layers ($\alpha \sim 5.6 \times 10^{-6}\ k^{-1}$) during cool down which tends to mask the grown-in tensile strain due to lattice mismatch. Most of the post-growth ex-situ strain characterizations [8-13] would in this case measure a combination of a tensile stress due to lattice mismatch and a compressive component due to thermal expansion mismatch. In an attempt to

https://doi.org/10.1557/S109257830000346X Published online by Cambridge University Press

isolate these two competing factors by directly probing the grown-in strain, we have employed an *in-situ* stress/strain monitor based on wafer-curvature measurement [14]. In this paper we will report the monitoring and subsequent control of grown-in strain of AlGaN on sapphire using different buffer layer schemes.

EXPERIMENT

A high-speed (1200 rpm), inductively heated, rotating disk reactor (RDR) was used to deposit GaN films (nominally 1-3 μm thick) onto 2" diameter, 330μm thick, (0001) sapphire wafers. Trimethylgallium, trimethylaluminum, and ammonia where used as the precursors, with hydrogen as the carrier gas. A detailed description can be found in Ref. [15]. A two-step deposition process was used. Initially, a LT buffer of GaN (~550^{o}C) or AlN (~600^{o}C) was grown. The buffer was then heated to 1050^{o}C and stabilized for 1 minute prior to deposition of the high temperature (HT) layer.

Real time wafer curvature measurements were performed with a multi-beam optical stress sensor (MOSS) [16] modified for use on our reactor. To determine the wafer curvature, the divergence of an array of initially parallel laser beams is measured on a CCD camera after reflection of the array from the film/substrate surface. Changes in wafer curvature induce a proportional change in the beam spacing on the camera. This technique provides a direct measurement of the stress during deposition and is described in detail in Ref. [17].

The relation between film stress (σ_f), and substrate curvature (k), is given by Stoney's equation [18],

$$s_f h_f = \frac{M_s h_s^2}{6} k \ , \qquad (1)$$

h_f and h_s are the film and substrate thickness, respectively and M_s is the substrate biaxial modulus. Curvature is directly proportional to the product of the film stress and film thickness ($s_f h_f$), both of which vary, in general, during growth. Equation 1 can be derived by balancing the forces and bending moments in the film with those in the substrate, and assuming the film is much thinner then the substrate [18]. We also simultaneously obtain information on the surface roughness and film thickness during deposition by monitoring the intensity of one of the reflected laser beams, similar to the method described in Ref. [19].

RESULTS AND DISCUSSION

Figure 3 shows the stress-thickness product ($s_f h_f$) and the reflected beam intensity as functions of growth time (see the following explanation) during growth of an AlGaN (Al~15%) layer on a 0.6 μm GaN layer grown at 1050°C. We have reported that [19] *in-situ* reflectance could provide the information of growth rate from the periodicity of Fabry-Perot interference. Such information in turn enables the conversion of time axis into film thickness (h_f). On a plot of $s_f h_f$ versus h_f, the slope is simply the grown-in stress (s_f). A positive slope on such a plot denotes a *tensile* stress throughout this paper.

A slight slope of the $s_f h_f$ curve during GaN growth (in Figure 3) was observed which suggests the presence of a slight tensile stress. The grown-in stress of GaN on sapphire is the subject of another publication [14]. After a growth transition in adjusting the reactor parameters for the growth of AlGaN (an artifact of an abrupt decrease in the $s_f h_f$ curve was therefore generated), a steady slope of 1.33 GPa was established which agrees well with the expected value

https://doi.org/10.1557/S109257830000346X Published online by Cambridge University Press

assuming a pseudomorphic growth. After the growth of approximately 0.6 μm of AlGaN, however, a step decrease of the $s_f h_f$ curve was recorded. Tentatively this feature is designated to be the relief of grown-in tensile stress due to the occurrence of cracking. (Cracking was indeed observed from Nomarski microscopy.) One implication is that the use of a thick GaN bottom layer, a common practice shared by the InGaN-based heterostructures, could lead to a build-up of excessive tensile strain in the case of AlGaN-based heterostructures for UV optoelectronics.

Direct growth of AlGaN on sapphire via LT buffer layers becomes attractive as a means to circumvent and alleviate the mismatch-induced tension imposed inevitably by the two-dimensional growth mode (i.e. AlGaN on a HT GaN layer). In Figures 4 and 5, $s_f h_f$ and reflectance versus thickness are presented for the growth of AlGaN (Al~17% in both cases) on LT GaN and AlN buffer layers, respectively, on sapphire substrates. Even though a tensile stress (0.82 GPa) was still measured for AlGaN on LT GaN buffer (Figure 4), it is interesting to note that this value is less than half of the expected stress due to the mismatch between $Al_{0.17}Ga_{0.83}N$ and GaN. One could speculate that the conventional, mismatch-induced strain constraint is somewhat relaxed under a possibly three-dimensional island growth mode.

In the case of direct growth of AlGaN on a LT AlN buffer (Figure 5), the $s_f h_f$ curve first moves downward, indicative of a *compressive* stress, before assuming a relatively flat (stress free) growth mode. The origin of the compressive strain during the initial growth of $Al_{0.17}Ga_{0.83}N$ is currently under investigation. A plausible cause is that the AlN nucleation template has a smaller lattice constant than that of AlGaN. The compressive stress was estimated to be around 1.3 GPa, much less than the full mismatch between $Al_{0.17}Ga_{0.83}N$ and AlN (around 9 GPa).

CONCLUSIONS

Using a novel *in-situ* stress monitor, we measured the grown-in strain of AlGaN on various layers. It was found that AlGaN grown on a thick HT GaN layer has a tensile strain well predicated by the pseudomorphic lattice mismatch before strain relaxation occurs. Growth on a LT GaN buffer layer resulted in a relaxation of more than 50% of the coherent tensile strain. The use of a LT AlN buffer caused a compressive strain during the initial (first 0.1 μm) growth of AlGaN. The combination of LT GaN and AlN buffer schemes could lead to the control of strain during AlGaN growth for UV optoelectronics.

ACKNOWLEDGMENTS

The authors gratefully acknowledge valuable interaction with H. Amano (Meijo University, Japan). Technical assistance by T. Kerley and J. Hunter is also acknowledged. Sandia is a multiprogram laboratory, operated by Sandia Corporation, a Lockheed Martin company, for the United States Department of Energy, under contract DE-AC04-94AL85000.

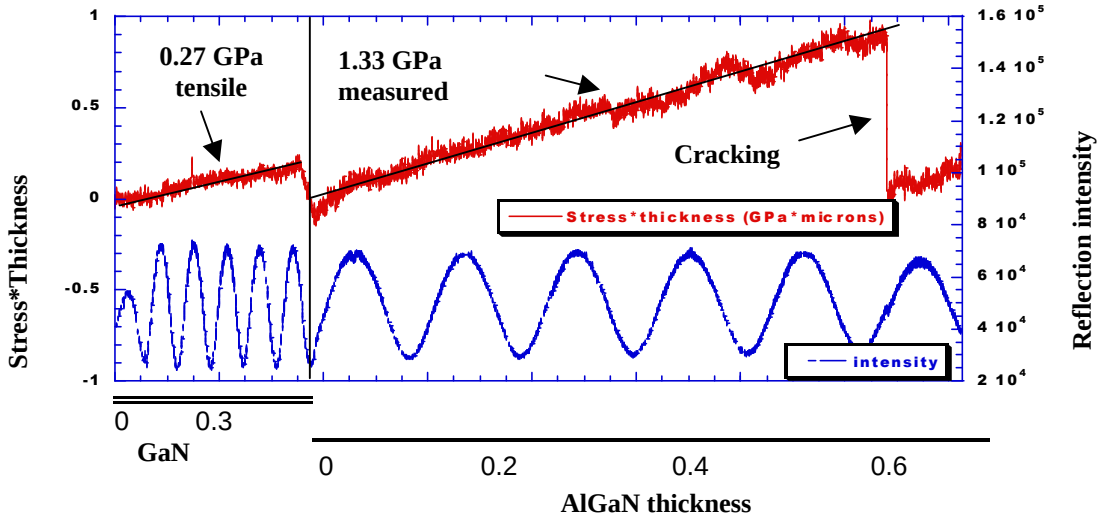

Figure 3 Stress-thickness product and reflectance versus thickness during growth of AlGaN (Al~0.15) on a 0.6 μm GaN layer

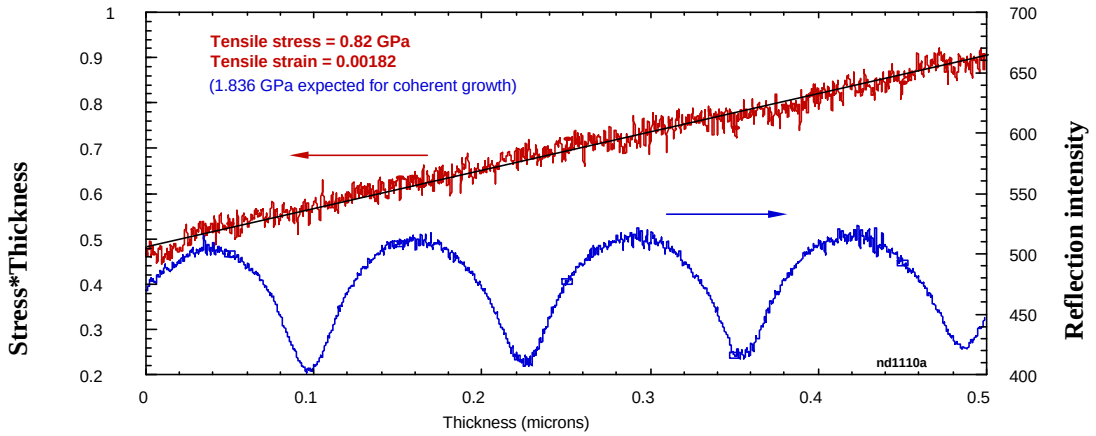

Figure 4 Stress-thickness product and reflectance versus thickness during growth of AlGaN (Al~0.17) directly on a LT GaN buffer on sapphire

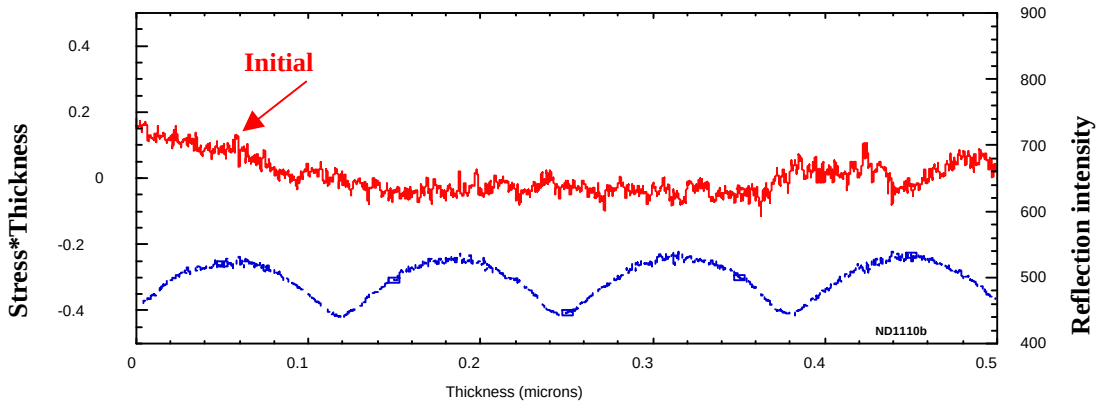

Figure 5 Stress-thickness product and reflectance versus thickness during growth of AlGaN (Al~0.17) directly on a LT AlN buffer on sapphire

https://doi.org/10.1557/S109257830000346X Published online by Cambridge University Press

REFERENCES

1. For a review, see S. Nakamura and G. Fasol, *The Blue Laser Diode*, Springer-Verlag, Berlin (1997).
2. A. Trampert, O. Brandt, and K. H. Ploog, *Gallium Nitride (GaN) I*, edited by J. I. Pankove and T. D. Moustakas, Academic Press, San Diego (1998), p167.
3. For example, C. Kisielowski, J. Kruger, S. Ruvimov, T. Suski, J. W. Ager III, E. Jones, Z. Liliental-Weber, M. Rubin, E. R. Weber, M. D. Bremser, and R. F. Davis, Phys. Rev. B 54, 17745 (1996).
4. T. Detchprohm, K. Hiromatsu, K. Itoh, and I. Akasaki, Jpn. J. Appl. Phys. 31, L1454 (1992)
5. J. Han, M. H. Crawford, R. J. Shul, J. J. Figiel, M. Banas, L. Zhang, Y. K. Song, H. Zhou, and A. V. Nurmikko, Appl. Phys. Lett, 73, 1688 (1998)
6. O. Gfrorer, T. Schlusener, V. Harle, F. Scholz, and A. Hangleiter, Mat. Res. Soc. Symp. Proc. 449, 429 (1997)
7. W. G. Perry, M. B. Bremser, T. Zheleva, K. J. Linthicum, and R. F. Davis, Thin Solid Films 324, 107 (1998).
8. W. Li, W. Ni, Appl. Phys. Lett. 68, 2705 (1996).
9. M. Leszczynski, T. Suski, H. Teisseyre, P. Perlin, I. Grzegory, J. Jun, S. Porowski, J. Appl. Phys 76, 4909 (1994).
10. T. Kozawa, T. Kachi, H. Kano, H. Nagase, N. Koide, K. Manabe, J. Appl. Phys. 77, 4389, (1995).
11. B. Skromme, H. Zhao, D. Wang, H. Kong, M. Leonard, G. Bulman, R. Molnar, Appl. Phys. Lett. 71, 829 (1997)
12. I. Lee, I. Choi, C. Lee, S. Noh, Appl. Phys. Lett. 71,1359, (1997)
13. P. Vennegues, B. Beaumont, M. Vaille, P. Gilbart, J. of Crystal Growth, 173, 249 (1997).
14. S. Hearne, E. E. Chason, J. Han, J. A. Floro, J. Figiel, J. Hunter , H. Amano, I. Tsong, Appl. Phys. Lett. 74, 356 (1999)
15. J. Han, T. B. Ng, R. M. Biefeld, M. H. Crawford, D. M. Follstaedt, Appl. Phys. Lett, 71, 3114 (1997)
16. C. Taylor, D. Barlett, E. Chason, J. A. Floro, Ind. Physicist 4, 25 (1998)
17. J. Floro, E. Chason, S. Lee, R. Twesten, R. Hwang, L. Freund, J. Elec. Mat. 26, 969 (1997)
18. M. Doerner and W. Nix, CRC Critical Reviews in Sol. State and Mat. Sci. 14, 224, (1988).
19. T. B. Ng, J. Han, R. M. Biefeld, and M. V. Weckwerth, J. Electron. Mat. 27, 190 (1998).

https://doi.org/10.1557/S109257830000346X Published online by Cambridge University Press